Single Transition-to-single Transition Polarization Transfer (ST2-PT) in [15N,1H]-TROSY

Journal Article

Author(s):
Pervushin, Konstantin V.; Wider, Gerhard; Wüthrich, Kurt

Publication date:
1998

Permanent link:
https://doi.org/10.3929/ethz-b-000422786

Originally published in:
Journal of Biomolecular NMR 12(2), https://doi.org/10.1023/A:1008268930690

Journal of Biomolecular NMR, **12:** 345–348, 1998.
KLUWER/ESCOM

Single transition-to-single transition polarization transfer (ST2-PT) in [^{15}N,^{1}H]-TROSY

Konstantin V. Pervushin, Gerhard Wider & Kurt Wüthrich[1]
Institut für Molekularbiologie und Biophysik, Eidgenössische Technische Hochschule Hönggerberg, CH-8093 Zürich, Switzerland

Received 13 March 1998, Accepted 10 April 1998

Key words: transverse relaxation-optimized spectroscopy, sensitivity enhancement, isotope labeled proteins

Abstract

This paper describes the use of single transition-to-single transition polarization transfer (ST2-PT) in transverse relaxation-optimized spectroscopy (TROSY), where it affords a $\sqrt{2}$ sensitivity enhancement for kinetically stable amide ^{15}N–^{1}H groups in proteins. Additional, conventional improvements of [^{15}N,^{1}H]-TROSY include that signal loss for kinetically labile ^{15}N–^{1}H groups due to saturation transfer from the solvent water is suppressed with the 'water flip back' technique and that the number of phase steps is reduced to two, which is attractive for the use of [^{15}N,^{1}H]-TROSY as an element in more complex NMR schemes. Finally, we show that the impact of the inclusion of the ^{15}N steady-state magnetization (Pervushin et al., 1998) on the signal-to-noise ratio achieved with [^{15}N,^{1}H]-TROSY exceeds by up to two-fold the gain expected from the gyromagnetic ratios of ^{1}H and ^{15}N.

Abbreviations: NMR, nuclear magnetic resonance; rf, radio-frequency; 2D, two-dimensional; FID, free induction decay; DD, dipole–dipole; CSA, chemical shift anisotropy; COSY, correlation spectroscopy; TROSY, transverse relaxation-optimized spectroscopy; PFG, pulsed field gradient; S/N, signal-to-noise ratio; *ftz* homeodomain, *fushi tarazu* homeodomain polypeptide of 70 amino acid residues, with the homeodomain in positions 3–62.

Rapid transverse relaxation in amide ^{15}N–^{1}H groups by dipole–dipole coupling (DD) and chemical shift anisotropy (CSA) modulated by rotational molecular motions limits the size of biomacromolecular structures that can be studied by NMR spectroscopy in solution. Transverse relaxation-optimized spectroscopy (TROSY) (Pervushin et al., 1997) uses spectroscopic means to reduce T_2 relaxation based on the fact that cross-correlated relaxation caused by interference of DD and CSA gives rise to different relaxation rates of the individual multiplet components in a system of two coupled spins $\frac{1}{2}$, I and S, such as, for example, the ^{15}N–^{1}H fragment of a peptide bond (Guéron et al., 1983; Goldman, 1984; Farrar and Stringfellow, 1996). Theory shows that at ^{1}H frequencies near 1 GHz highly efficient cancellation of transverse relaxation effects within the ^{15}N–^{1}H moiety can be achieved for one of the four multiplet components (Pervushin et al., 1997). TROSY observes exclusively this narrow component, for which the residual linewidth is then mainly due to DD interactions with remote hydrogen atoms in the protein, and possibly to conformational exchange terms. This communication describes further improvements of the TROSY experimental scheme with the use of a new principle, single transition-to-single transition polarization transfer (ST2-PT), and some established tricks of the trade.

Since TROSY deals with the individual components of a multiplet it is best described in the basis of the single-transition operators referring to the transitions 1→2 and 3→4 of spin S, and 1→3 and 2→4 of spin I for a system of two spins $\frac{1}{2}$, with the corresponding precession frequencies (Pervushin et al., 1997):

$$I_{13}^{\mp} = I^{\mp}/2 + I^{\mp}S_z \qquad \omega_I^{13} = \omega_I + \pi J_{IS}, \quad (1)$$

[1]To whom correspondence should be addressed.

$$I_{24}^{\mp} = I^{\mp}/2 - I^{\mp}S_z \qquad \omega_I^{24} = \omega_I - \pi J_{IS}, \quad (2)$$

$$S_{12}^{\mp} = S^{\mp}/2 + I_z S^{\mp} \qquad \omega_S^{12} = \omega_S + \pi J_{IS}, \quad (3)$$

$$S_{34}^{\mp} = S^{\mp}/2 - I_z S^{\mp} \qquad \omega_S^{34} = \omega_S - \pi J_{IS}. \quad (4)$$

The corresponding Cartesian single-transition operators are defined accordingly. Since the phases of the rf-pulses and the receiver have a direct influence on the analysis of the spin dynamics of single transitions, the following calculations use the definitions reviewed by Levitt (1997). For example, the phases of all rf-pulses and the receiver phase, ϕ, are sensitive to the gyromagnetic ratio, γ, and are used in the calculations in the place of the 'raw' phase ψ specified in the spectrometer pulse program and listed in Figure 1, where $\phi = (-\gamma/|\gamma|)\psi$.

The evolution of the density operator in the original TROSY experiment (Pervushin et al., 1997) can be schematically represented as:

$$I_y^{13} + I_y^{24} \rightarrow S_x^{34}\cos(\omega_S^{34}t_1) \rightarrow I_x^{24}\cos(\omega_S^{34}t_1) \quad (5)$$

The first arrow designates coherence transfer from ^{1}H to ^{15}N and ^{15}N chemical shift evolution during the delay t_1, and the second arrow represents the coherence transfer from ^{15}N to ^{1}H. Correspondingly, $S_y^{34}\sin(\omega_S^{34}t_1)$, which is required for phase-sensitive recordings in the ^{15}N dimension, is selected in alternate scans, so that in each individual application of the pulse sequence only half of the ^{15}N magnetization, i.e., either S_x^{34} or S_y^{34}, is transferred to the data acquisition. When compared to the corresponding part of an earlier version of the [^{15}N,^{1}H]-TROSY scheme (Figure 1 in Pervushin et al., 1997) the ST2-PT element (box in the experimental scheme of Figure 1) uses a different phase cycling scheme for the rf-pulses, which, when combined with application of the echo/anti-echo quadrature detection method (Palmer III et al. 1991; Cavanagh and Rance, 1993; Kay et al., 1992; Muhandiram et al., 1993; Schleuchter et al., 1993, 1994) in the ^{15}N dimension, permits phase-sensitive detection of the desired ^{15}N doublet component. ST2-PT thus enables simultaneous transfer of S_x^{34} and S_y^{34} to I_{24}^{-}, and thus transfers the total magnetic polarization of the 1→2 transition of spin S to the 1→3 transition of spin I, and the total polarization of the 3→4 transition of S to the 2→4 transition of I:

$$S_x^{12} \pm i S_y^{12} = S_{12}^{\pm} \rightarrow I_{13}^{\pm} \quad (6)$$

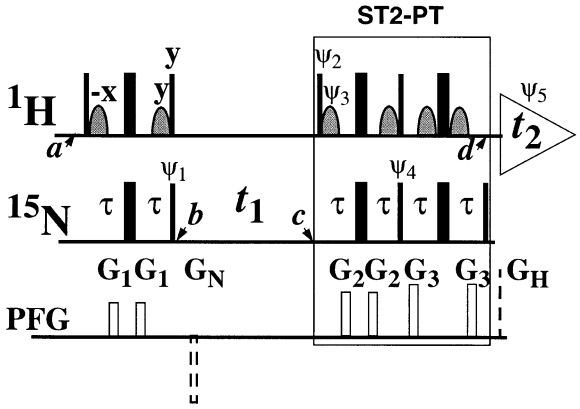

Figure 1. Experimental scheme for 2D [^{1}H,^{15}N]-TROSY using single transition-to-single transition polarization transfer (box labeled ST2-PT). On the lines marked ^{1}H and ^{15}N, narrow and wide bars stand for non-selective 90° and 180° radio-frequency pulses, respectively. The delay $\tau = 2.7$ ms. The line marked PFG indicated the pulsed magnetic field gradients applied along the z-axis: G_1, amplitude 30 G/cm, duration 1 ms; G_2, 40 G/cm, 1 ms; G_3, 48 G/cm, 1 ms; G_N, −60 G/cm, 0.75 ms; G_H, 60 G/cm, 0.076 ms. The following two-step phase cycling scheme was used: $\psi_1 = \{y, -x\}$; $\psi_2 = \{-y\}$; $\psi_3 = \{y\}$; $\psi_4 = \{-y\}$; ψ_5(receiver) $= \{y, -x\}$; x on all other pulses. To obtain a complex interferogram a second FID is recorded for each t_1 delay, with $\psi_1 = \{y, x\}$; $\psi_2 = \{y\}$; $\psi_3 = \{-y\}$; $\psi_4 = \{y\}$, and G_N inverted. The use of ST2-PT thus results in a 2D [^{1}H,^{15}N]-correlation spectrum that contains only the most slowly relaxing component of the 2D ^{15}N–^{1}H multiplet. The data are processed as described by Kay et al. (1992). Water saturation is minimized by keeping the water magnetization along the $+z$-axis during the entire experiment, which is achieved by the application of the water-selective 90° rf-pulses indicated by curved shapes on the line ^{1}H. The use of the gradients G_N and G_H (broken lines) allows the recording of the pure phase absorption spectrum without any cycling of the pulse phases. This may be attractive, for example, to minimize the recording time of the experiment, but the first point of the FIDs must then be back-predicted in both dimensions. Alternatively, when the two-step phase cycle is employed, the gradients G_N and G_H are usually not applied.

$$S_x^{34} \pm i S_y^{34} = S_{34}^{\pm} \rightarrow I_{24}^{\mp}. \quad (7)$$

When both pathways indicated by Equations (6) and (7) are retained, two diagonally shifted signals represent two out of the four ^{15}N–^{1}H multiplet components in the resulting [^{15}N,^{1}H]-correlation spectrum. The undesired polarization transfer pathway, $S_{12}^{\pm} \rightarrow I_{13}^{\pm}$, is suppressed either by two-step cycling of the phases ψ_1 and ψ_5 (Figure 1), or by application of PFGs during t_1 and at time point d (Figure 1). The remaining anti-echo polarization transfer pathway, $S_{34}^{+} \rightarrow I_{24}^{-}$, connects a single transition of spin S with a single transition of spin I, and in alternate scans with inversion of the rf-phases ψ_2 and ψ_4, the corresponding echo transfer, $S_{34}^{-} \rightarrow I_{24}^{-}$, is recorded. Thus,

the overall magnetization transfer pathway of the experiment of Figure 1 can schematically be represented as:

$$I_y^{13} + I_y^{24} \rightarrow S_{34}^{+} \exp(-i\omega_S^{34} t_1) \rightarrow I_{24}^{-} \exp(-i\omega_S^{34} t_1). \quad (8)$$

The sensitivity of [^{15}N,^{1}H]-TROSY observation of kinetically stable amide ^{15}N–^{1}H groups in proteins is thus enhanced by a factor $\sqrt{2}$, when compared with the experimental scheme of Figure 1 in Pervushin et al. (1997). In conventional, heteronuclear correlation experiments a similar selection of two coherence transfer pathways, $I_z S^{+} \rightarrow I^{-}$ and $I_z S^{-} \rightarrow I^{-}$, has previously been introduced to increase sensitivity (Palmer III et al., 1991; Cavanagh and Rance, 1993; Kay et al., 1992; Muhandiram et al., 1993; Schleuchter et al., 1993, 1994).

The TROSY experimental scheme in Figure 1 prevents saturation of the water magnetization during the pulse sequence (Kay et al., 1994; Stonehouse et al., 1994; Jahnke and Kessler, 1994) with the use of 'water flip back' pulses (Grzesiek and Bax, 1993). The two water-selective pulses during INEPT ensure that the water magnetization is along $+z$ at time point b. During the ST2-PT element the water magnetization is treated similarily, so that it is aligned along the $+z$ axis at time point d and during acquisition. The WATERGATE element (Piotto et al., 1992) immediately before d (Figure 1) is used to suppress residual water magnetization in the transverse plane before data acquisition. In this way, loss in signal amplitude for kinetically labile ^{15}N–^{1}H groups by transfer of saturation from the solvent water is largely suppressed.

For experimental verification of the predicted gain in sensitivity by the use of ST2-PT we compared spectra recorded either with the experimental scheme of Figure 1 or with the original TROSY experiment (Pervushin et al., 1997). [^{15}N,^{1}H]-correlation spectra were measured with the ^{15}N-labeled 70-residue *fushi tarazu* homeodomain in a 17 kDa complex with a 14-base operator DNA fragment (Percival-Smith et al., 1990; Qian et al., 1994). Figure 2 shows cross sections parallel to the ω_2(^{1}H) axis through the ^{15}N–^{1}H correlation spectra, showing the ^{15}N–^{1}H cross peak of Ala 35 in the two spectra. The gain in signal-to-noise ratio for this resonance when using the ST2-PT element was about 1.5, and a similar gain in sensitivity was observed for the other ^{15}N–^{1}H cross peaks in the *ftz* homeodomain–DNA complex.

In the experiments of Figure 2 we used both the ^{1}H and ^{15}N steady-state magnetizations (Pervushin et al., 1998). The product operator analysis (Sørensen et al., 1983) accounts for this by the following density matrix at time b in the experimental scheme of Figure 1:

$$\sigma_b = i\frac{u+v}{2}(S_{12}^{-} - S_{12}^{+}) - i\frac{u-v}{2}(S_{34}^{-} - S_{34}^{+}). \quad (9)$$

The constant factors u and v reflect the relative magnitudes of the steady-state ^{1}H and ^{15}N magnetizations, respectively, which are determined by the gyromagnetic ratios, the spin-lattice relaxation rates and the delay between individual data recordings (Ernst et al., 1987). Since the $S_{34}^{\pm}$ operators are transferred to observable magnetization, both the ^{1}H and ^{15}N steady-state magnetizations add up to the signal obtained with the pulse sequence of Figure 1, which is proportional to $\frac{1}{2}(u - v)$. To assess the contribution from the ^{15}N steady-state magnetization, a spectrum measured with the experimental scheme of Figure 1 was compared with an experiment using the same setup, except that the phase of the second 90°(^{1}H) pulse and the preceding water-selective pulse was $-y$. The resulting signal

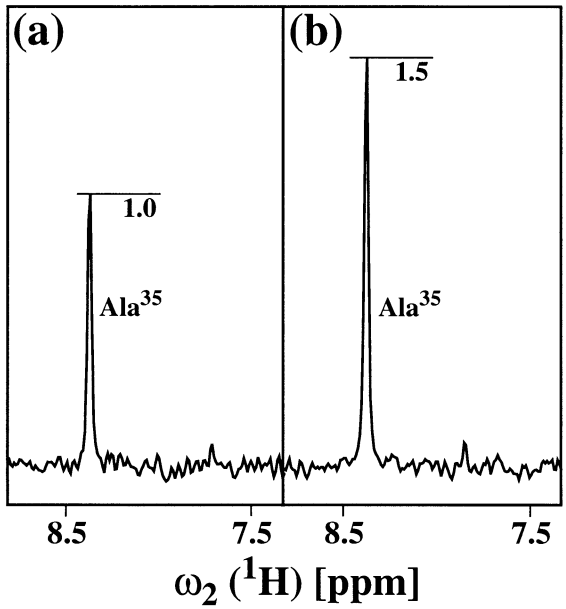

Figure 2. Cross sections parallel to the ω_2 axis through the ^{15}N–^{1}H cross-peak of Ala 35 in [^{1}H,^{15}N]-TROSY spectra. (a) [^{1}H,^{15}N]-TROSY recorded with the experimental scheme of Figure 1 in Pervushin et al. (1997); (b) [^{1}H,^{15}N]-TROSY recorded with the pulse scheme of Figure 1, using ST2-PT. The experiments were performed with a 2 mM solution of the uniformly ^{15}N-labeled *ftz* homeodomain in a 17 kDa complex with an unlabeled 14-bp DNA duplex in 95% H_2O/5% $^{2}H_2O$ at 25 °C, pH = 6.0, at a ^{1}H frequency of 750 MHz. The measuring time, the experimental setup and the processing parameters were identical for the two experiments. The relative peak amplitudes are indicated.

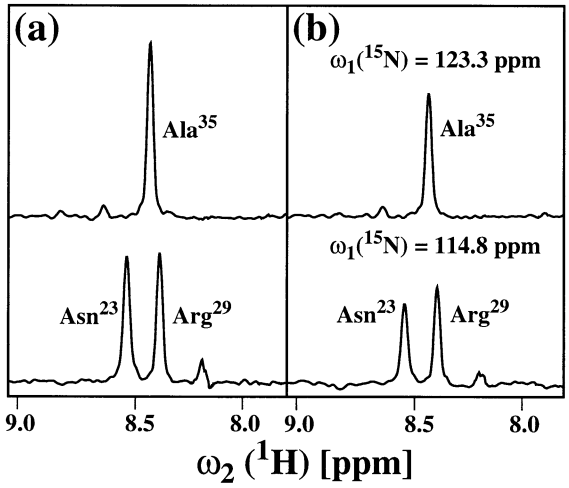

Figure 3. Contribution to the signal intensity from the ^{15}N steady-state magnetization in [^{15}N,^{1}H]-TROSY. (a) Spectrum recorded with the experimental scheme of Figure 1. (b) Spectrum recorded using the experimental scheme of Figure 1 with the phase of the second 90°(^{1}H) pulse and the preceding water-selective pulse set to $-y$. The measuring time and processing parameters were identical for both spectra, which were recorded at 750 MHz with the same sample as in Figure 2. The cross sections parallel to the ω_2(^{1}H) axis show the ^{15}N–^{1}H spin systems of Ala 35 (upper traces), and of Asn 23 and Arg 29 (lower traces).

amplitudes correspond, respectively, to the amplitude from the ^{1}H steady-state magnetization plus and minus the contribution from the ^{15}N steady-state magnetization. For the ^{15}N–^{1}H groups of Ala 35, Asn 23 and Arg 29 the ratios of the signal amplitudes in the two spectra were 1.4, 1.5 and 1.3 respectively (Figure 3). Thus, in these three signals the ^{15}N steady-state magnetization provides 17%, 21% and 11%, respectively, of the signal intensity obtained from the ^{1}H steady-state magnetization alone. These numbers represent up to two-fold higher enhancement than expected on the basis of the different gyromagnetic ratios for ^{1}H and ^{15}N, which reflects the faster T_1 relaxation for ^{15}N nuclei than for ^{1}H under the conditions of these experiments (data to be published).

Acknowledgements

Financial support was obtained from the Schweizerischer Nationalfonds (project 31.49047.96). We thank M. Wahl for the preparation of the *ftz* homeodomain–DNA complex.

References

Bodenhausen, G. and Ruben, D.J. (1980) *Chem. Phys. Lett.* **69**, 185–189.
Farrar, T.C. and Stringfellow, T.C. (1996) in *Encyclopedia of NMR*, Grant, D.M. and Harris, R.K. (eds.), Wiley, New York, Vol. **6**, pp. 410–4107.
Cavanagh, J. and Rance, M. (1993) *Ann. Rev. NMR Spectrosc.* **27**, 1–58.
Goldman, M. (1984) *J. Magn. Reson.* **60**, 437–452.
Grzesiek, S. and Bax, A. (1993) *J. Biomol. NMR.* **3**, 627–631.
Guéron, M., Leroy, J.L. and Griffey, R.H. (1983) *J. Am. Chem. Soc.* **105**, 7262–7266.
Jahnke, W. and Kessler, H. (1994) *J. Biomol. NMR.* **4**, 735–739.
Kay, L.E., Keifer, P. and Saarinen, T. (1992) *J. Am. Chem. Soc.* **114**, 10663–10665.
Kay, L.E., Xu, G.Y. and Yamazaki, T. (1994) *J. Magn. Reson. A* **109**, 129–132.
Levitt, M.H. (1997) *J. Magn. Reson.* **126**, 164–182.
Muhandiram, D.R., Xu, G.Y. and Kay, L.E. (1993) *J. Biomol. NMR* **3**, 463–470.
Müller, L. (1979) *J. Am. Chem. Soc.* **101**, 4481–4484.
Palmer III, A.G., Cavanagh, J., Wright, P.E. and Rance, M. (1991) *J. Magn. Reson.* **93**, 151–170.
Percival-Smith, A., Müller, M., Affolter, M. and Gehring, W.J. (1990) *EMBO J.* **9**, 3967–3974.
Pervushin, K., Riek, R., Wider, G. and Wüthrich, K. (1997) *Proc. Natl. Acad. Sci. USA* **94**, 12366–12371.
Pervushin, K., Riek, R., Wider, G. and Wüthrich, K. (1998) *J. Am. Chem. Soc.* **120**, 6394–6400.
Piotto, M., Saudek, V. and Sklenar, V.J. (1992) *J. Biomol. NMR* **2**, 661–665.
Qian, Y.Q., Furukubo-Tokunaga, K., Resendez-Perez, D., Müller, M., Gehring, W.J. and Wüthrich K. (1994) *J. Mol. Biol.* **238**, 333–345.
Schleuchter, J., Sattler, M. and Griesinger, C. (1993) *Angew. Chem. Engl. Ed.* **32**, 1489–1491.
Schleuchter, J., Schwendinger, M.G., Sattler, M., Schmidt, P., Glaser, S.J., Sørensen, O.W. and Griesinger, C. (1994) *J. Biomol. NMR* **4**, 301–306.
Sørensen, O.W., Eich, G.W., Levitt, M.H., Bodenhausen, G. and Ernst R.R. (1983) *Prog. NMR Spectrosc.* **16**, 163–192.
Stonehouse, J., Shaw, G.L., Keeler, J. and Laue, E.D. (1994) *J. Magn. Reson. A* **107**, 178–182.